



3D Model Reconstruction of Blood Vessels in The Retina with Tubular Structure

Guedri Hichem, Fraj Chouchene, and Hafedh Belmabrouk

Faculty of Science Monastir,
Electronic and microelectronics laboratory LAB IT 06,
University of Monastir, Tunisia.

Abstract: We present in this paper a geometric interpretation of the 3D model reconstruction of the blood vessel of the human retina. The proposed method combines the approach of the vessel tracking algorithm with the use of a continuous model of generalized cylinder. The model is composed of two geometric objects: a generator axis H and a surface S , represented as a stack of contours plans attached to this axis. The segmentation algorithms by monitoring vessels that we propose is written by the use of three interpolation method for have a smooth generator axis H . First, the graph topology of the blood vessel is extracted from the human retina image. This is done after the skeletonisation of the image, then, the pixel classification (termination points and bifurcation points and inner points) and determination of the branches curve. Secondly, we use three methods of the approximation of the vessels for have a smooth curve (linear, cubic splines and least square linear interpolation). Afterwards, the construction of a 3D model from a vascular image is done by using the Right Generalized Cylinder State Model (RGC-sm). Finally, in a last part, we present results of segmentation and 3D reconstruction of a blood vessel group.

Keywords: 3D reconstruction, tubular structure, Right Generalized Cylinder, least square, linear spline, cubic spline, retinal blood vessel image.

1. Introduction

This manuscript is dedicated to studying and develop a general methodology to detect, analyze, visualize and reconstruct the 3D model of the blood vessels in the human retinal images [1-11]. We chose a segmentation approach by vessel tracking for the construction of a continuous cylindrical representation of the interest blood vessel, our method combines the sequential approach vessel tracking [12-14], with the use of a continuous model of a generalized cylinder. By its nature, the vessel tracking provides access to successive cross sections. The selected cylinder model [15-16] based on the state formalism, the model consists of two geometric objects: a generator axis H [17-22] and a surface S , represented as a stack of contours plans attached to this axis.

To quantify the degree of accuracy, we studied all stages of the approach (acquisition, segmentation and interpolation) that influence the accuracy.

The manuscript begins with a description of the problem proposal and the proposed algorithm. Then, we studied the Skeletonization of retina images [23-25] and the curve points are classified in several categories [26-28], namely endpoints, bifurcation points and interior points, (branches, crossover...). In the section 3, we are interested in the approximation of the vessels that are already extracted. To have a smooth curve, three methods of interpolation are used [29-31], namely least square, linear spline and cubic spline. Then we calculated the error induced by each method [32-34]. Section 4 presents the status of the generalized cylinder model, known as the RGC-sm (Right Generalized Cylinder State Model) [15-16], which we use in this work. Finally, section 5 presents results of segmentation and reconstruction of the 3D model of the human retinal blood vessels.

Received: March 9th, 2015. Accepted: December 16th, 2015

DOI: 10.15676/ijeel.2015.7.4.14

2. Problem proposal

Our objective is to extract data from a 2D image of the human retina by image segmentation [23-28]. In a second step, an interpolation curve of the blood vessel will be necessary to obtain a smooth axis H [29-31]. The analysis of the results is used to make a 3D reconstruction model of these vessels [9-11] by using the Right Generalized Cylinder State Model (RGC-sm) [15–16], which is the final step. Figure 1 exhibits the block diagram of the approach adopted.

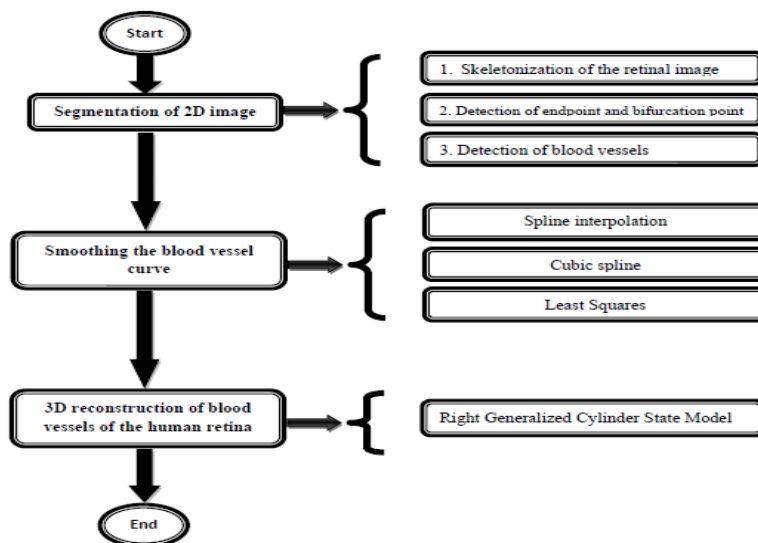


Figure 1. Block diagram

3. Image segmentation

After creating a binary version of the image using a global threshold automated method to locate and exhibit the blood vessels in the background images of the retina [23-25]. It is then modified with a series of morphological operators.

A. The skeleton

Skeletonization is an important process in the 2D image analysis. It helps to shorten the shape of an object and extract geometric features. The skeleton picture preserves connectivity and retains the topology of the original image but it reduces the width of objects to a unit thickness. This reduction allows better characterizing the image and better exploring [24].

B. Detection of endpoints and bifurcation points

This method determines the location of the endpoints and bifurcation points in the binary original image skeletonized [26-27].

1. The first step is to extract all the coordinates of all the pixels containing the information in the skeletonized image.
2. Select the coordinates of the current pixel to be tested and determine the coordinates of the eight neighboring pixels.
3. If this pixel has only one neighbor, then it is an end point and it will be saved in the matrix of the endpoints (Figure 2).

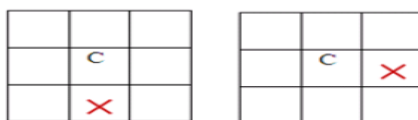


Figure 2. End point

- Otherwise, if the pixel has three or more neighbors, then it is a bifurcation point and it will be recorded (Figure 3).

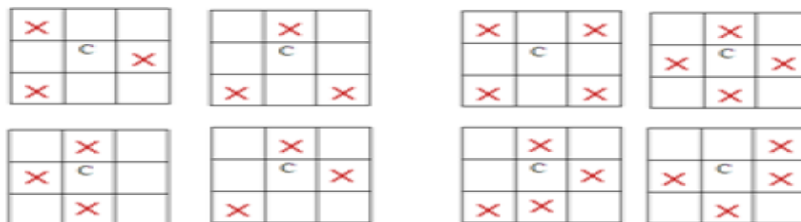


Figure 3. Bifurcation point

C. Detection point centerline of the blood vessels

First, we will choose the first endpoint E1 coordinates (m, n). Then we will check its 8 neighbors. We will find only a single pixel containing information V1 (since E1 is an endpoint). Then, we remove E1 and V1 is takes as the current point of the new test. This operation is repeated until a bifurcation point is detected. Then we apply the same process to the next endpoint [17-19] [27-28].

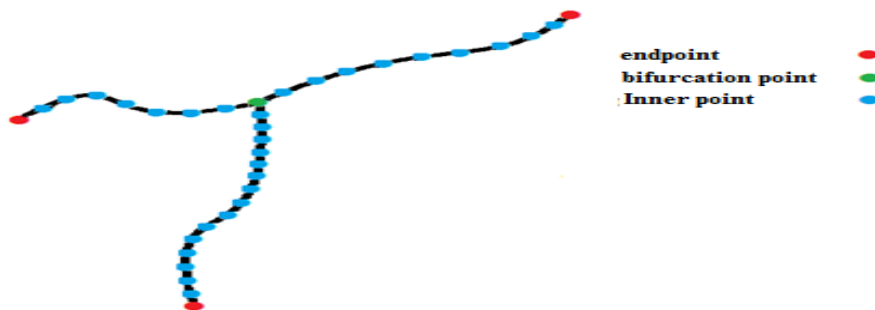


Figure 4. Inner point

4. Curve Blood vessel interpolation

There are many methods of interpolation .in this paper; we will test the performances of linear, cubic splines and least square linear regression [29-31]:

We dispose a set of n+1 Points $(x_i, y_i), i = 0, \dots, n$ such as $x_0 < x_1 < \dots < x_n$.

- Linear splines:

$$S(x) = \begin{cases} S_0(x) = a_0x + b_0, & x \in [x_0, x_1] \\ S_1(x) = a_1x + b_1, & x \in [x_1, x_2] \\ \vdots \\ S_{n-1}(x) = a_{n-1}x + b_{n-1}, & x \in [x_{n-1}, x_n] \end{cases} \quad (1)$$

- cubic splines:

$$S(x) \begin{cases} S_0(x) = a_0x^3 + b_0x^2 + c_0x + d_0, & x \in [x_0, x_1] \\ S_1(x) = a_1x^3 + b_1x^2 + c_1x + d_1, & x \in [x_1, x_2] \\ \vdots \\ S_{n-1}(x) = a_{n-1}x^3 + b_{n-1}x^2 + c_{n-1}x + d_{n-1}, & x \in [x_{n-1}, x_n] \end{cases} \quad (2)$$

- least square interpolation :

The model function $f(x, \beta)$ is set by $m \beta_1 \dots \beta_m$ parameters contained in the vector β . The minimum of a sum of squares (3)

$$S(\beta) = \sum_{i=1}^n (y_i - f(x_i, \beta))^2 \quad (3)$$

Is seeking where the gradient of S is 0 whether

$$\frac{\partial S(\beta)}{\partial \beta_k} = -2 \sum_{i=1}^n (y_i - f(x_i, \beta)) \frac{\partial f(x_i, \beta)}{\partial \beta_k} = 0 \quad k = 1, \dots, m$$

The interpolation error may be estimated by either the absolute value of the maximal error or by the standard deviation (rms value) of the error [32-34]:

$$\Delta f_{max} = \max_{i=1:N} |f_i - f'_i| \quad (4)$$

$$\sigma = \sqrt{\frac{1}{N} \sum_{i=1}^N (f_i - f'_i)^2} \quad (5)$$

5. 3D reconstruction

Our method uses the natural shape of the blood vessel: a vessel has a cylindrical shape which can be represented as a combination of an axe and a surface [14-16]. The interpolated curve is assumed to be the blood vessel axis [17-21], then for creating the cylindrical shape we need a set of successive 3D circles (Figure.5).

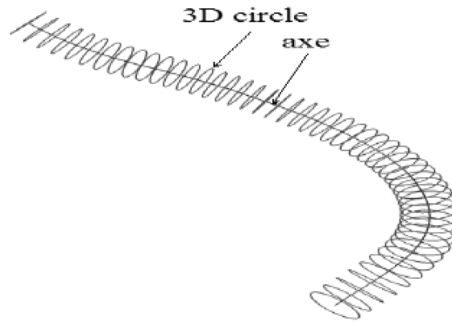


Figure 5. The axis H and the stack of contours of the surface

We start by defining the classic circle parameterization, a circle that has a center O (x₀, y₀) and radius r and has the parametric equation (6):

$$\begin{cases} X(t) = x_0 + r * \cos(\theta) \\ Y(t) = y_0 + r * \sin(\theta) \\ Z(t) = r * \sin(\theta) \end{cases} \quad \text{With } \theta \in [0:2\pi] \quad (6)$$

Then a surface reconstruction process is applied to the interpolated curve to obtain a representation of 3D blood vessel by using the Right Generalized Cylinder State Model (RGC-sm). the reconstruction is made piece-wise (figure 5) [15-16]. Indeed, we start with the first portion of the generalized cylinder whose center is defined by the end point P then P+1 [17-20], then we continue with the next part of the axe till the last point. With this method can determine the coordinates of the points P (x, y, z).

Right generalized cylinder:

Right generalized cylinder (RGC) is composed of two geometric objects: the first is a generator axis H which represents elongated shape of the vessel, and the second is a surface S which represents the vessel wall, a schematic of this presentation is presented in Figure 6 [15-16].

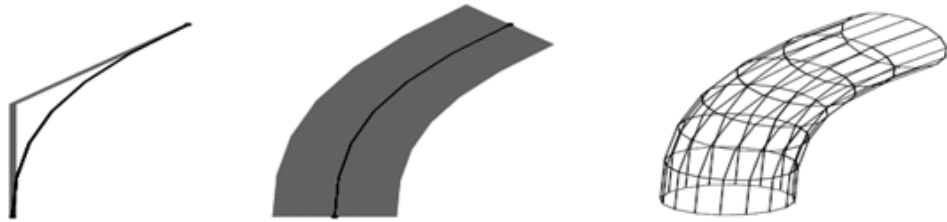


Figure 6. Presentation includes both geometric objects of the generalized right cylinder (RGC)

A RGC equation (7) should include a coupling of an ordinary axis H and a regular surface S and which may be represented by the pair of parametric equations:

$$\begin{cases} H = h(l): R^+ \rightarrow R^3 \\ S = s(l, w): R^+ \times R^+ \rightarrow R^3 \end{cases}, 0 \leq l \leq n \quad (7)$$

Where:

l is the axial parameter.

n is the axis' length.

w is the surface azimuthal parameter.

So the RGC formula (8), we introduce a radius parameter r to represent the cylinder as a volumetric object (figure 7):

$$C(l, w, r): R^+ \times R^+ \times R^+ \rightarrow R^3 \quad (8)$$

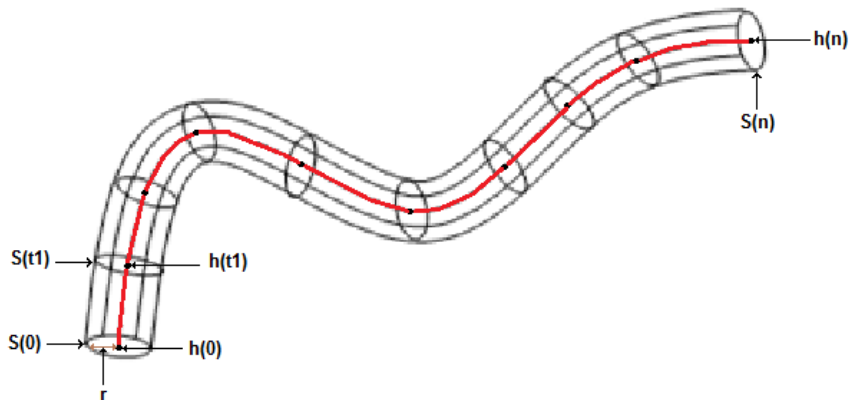


Figure 7. Scheme of RGC's equation parameters. Representation consists of the cylinder surface and its axis.

6. Result and discussion

We have used the stare database images [25], the reconstruction time takes into account the time required for image segmentation and the time needed for the reconstruction 3D. All these results were obtained on a workstation equipped with an Intel Pentium B960 CPU @ 2.20 GHz and 4GB of RAM processor.

A. Image segmentation of the human retina

The skeletonized image reduces the spaces occupied by the blood vessel to a line. On the skeleton so obtained (Figure 8b), we can define: the total number of bifurcation points, the end points and the inner points which are used to extract the vascular curve. We obtain for image im0002.jpg (Figure 8a), 63 end points (Figure 8c) and 185 bifurcation points (Figure 8d).

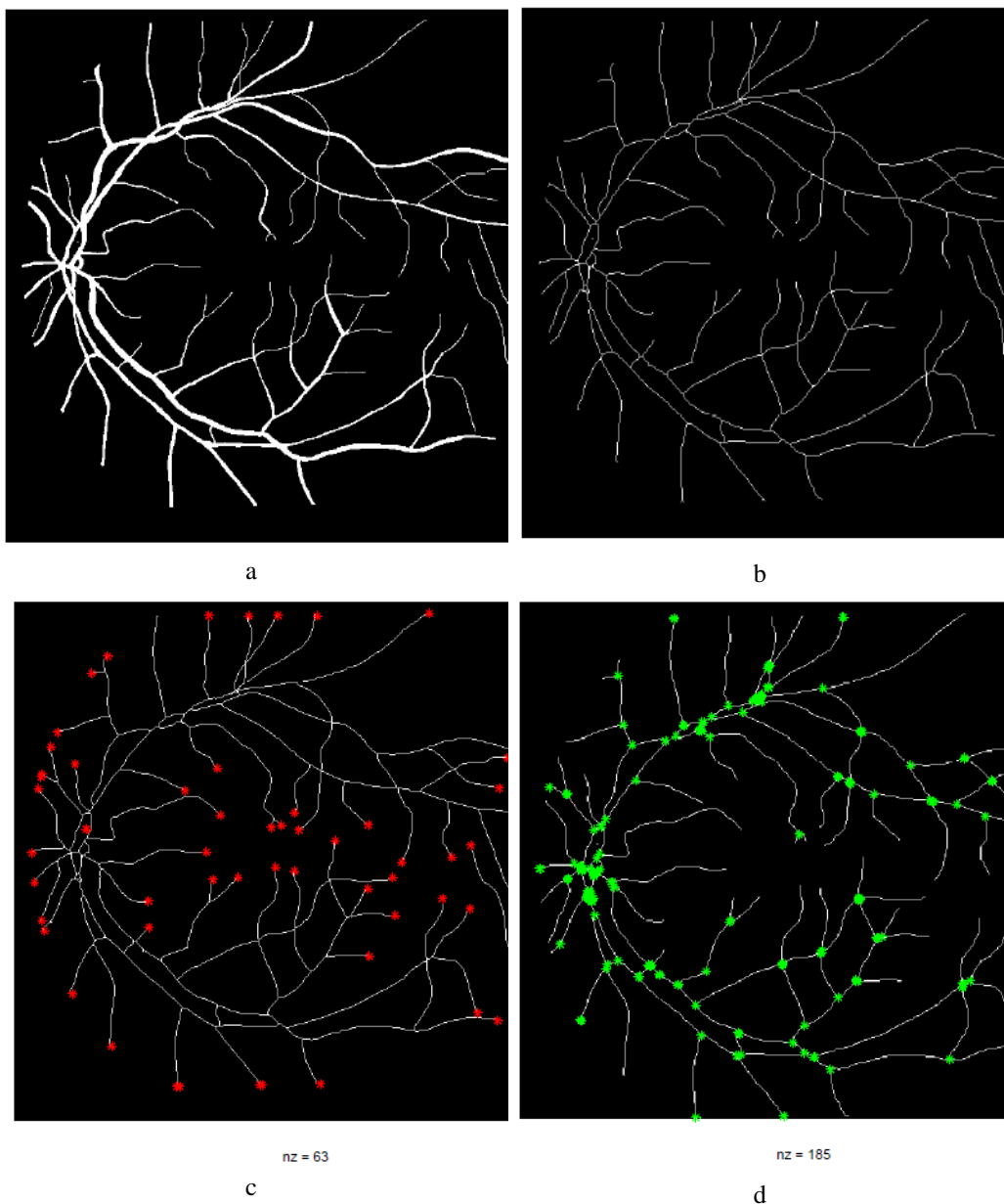


Figure 8 (a) Image 'im0002.JPG', (b) Skeletonization of the image 'im0002.JPG', (c) Endpoint, (d) Bifurcation points

B. Interpolation and error calculation

After the execution of the interpolating algorithm based on spline, least square or cubic spline we calculated the absolute error (4) and the standard deviation (rms) (5) for each one of these interpolations methods.

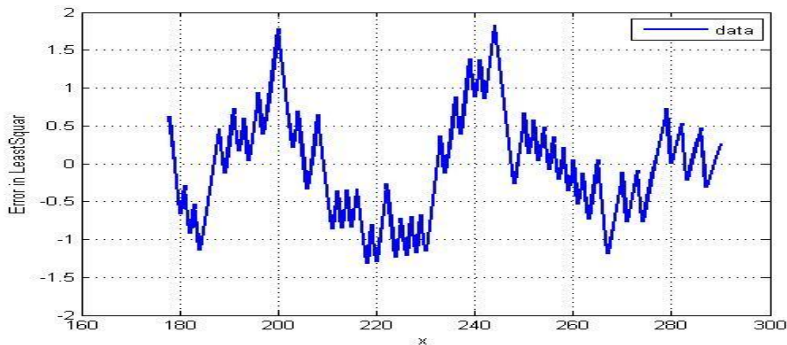


Figure 9. Error least squares interpolation.

Table 1. Calculated error

	Least squares interpolation	Spline interpolation	Cubic spline interpolation
Error absolute	1.8613	≈ 0	0
Rms	0.6967	≈ 0	0

Figure 9 present the error due to interpolation using the last square method for an example of blood vessel curve. The fluctuates in a random manner. The fluctuations are characterized by the maximal absolute error and rms value.

The results are recapitulated in table1 for the tree interpolation methods. The last square method gives rise to an important error. Indeed, the rms value is about 0.7 pixels and the maximal error is about 1.9 pixels. However, the interpolation errors vanish using the linear spline or the cubic spline .for this reason, in next step we will use the cubic spline interpolation. The 2D interpolation algorithm works perfectly, especially for the last two methods. If we compare the simulation results obtained with the results of Melissa Jourdain et al. [9] It may be noted that the results obtained by their methods proposed for the two sets of synthesized and ghost data show that the RMS error is 0.75, with a minimum error of 0 pixels and a maximum of 2 pixels. On the other hand, the results obtained after the simulation of monitoring methods used shows that the RMS error is 0.7 pixel for the method of Least squares and almost zero for the other two methods with an error of 1.8 pixels 0 the first method and 0 for the second and third method which is the superiority and reliability of the algorithm used.

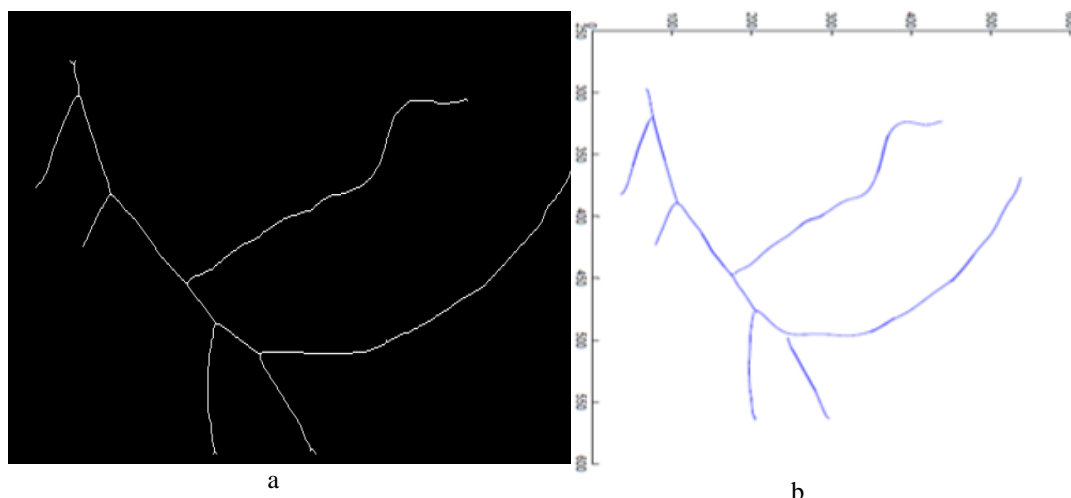


Figure 10. (a) The original blood vessel, (b) Interpolation by cubic spline

Figure 10 (a) shows the original blood vessel taken from the image 0002.jpg and Figure. 10 (b) presents the curve interpolation using cubic spline method. It is clear that the two images are identical and interpolation does not introduce any bias. We can consider that this step of the reconstruction of blood vessel axis has been made successfully.

C. 3D Reconstruction

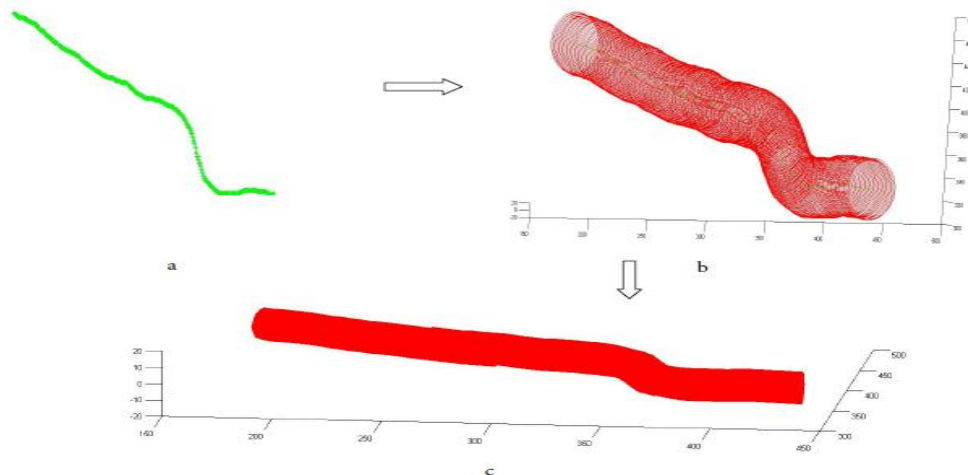


Figure 11. The different stages of the reconstruction of a blood vessels 3D model. (a) Shows the axis H. (b) the stack of contours constructing the surface. (c) 3D reconstruction of blood vessel.

Figure 11 shows a graphical interpretation of the method used for the reconstruction of a 3D model of blood vessel.

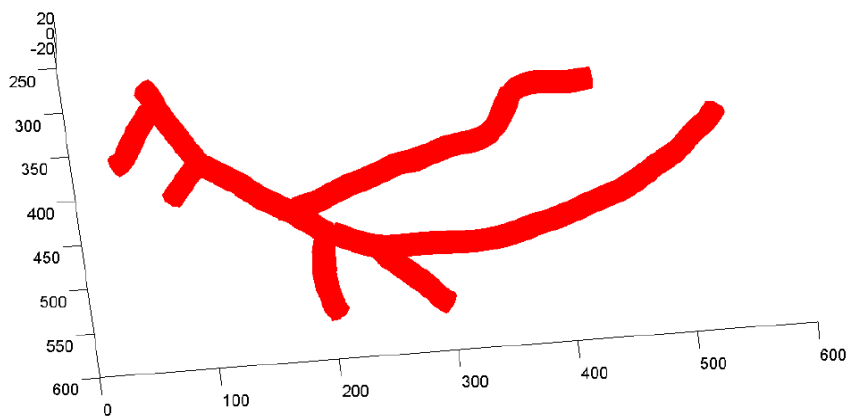


Figure 12. Reconstruction 3D of the blood vessel

The aim is not only to make a 3D reconstruction for visualization purposes but also to describe the shape of the structure studied by one or more geometric objects such as implicit surfaces, parametric surfaces or freeform surfaces. The benefits of this approach to perform 3D reconstruction by generalized cylinder method are: first in time is the precision of description of the form. Then it allows us naturally integrates the sequential monitoring concept, as it allows the definition of a set of analytical measurements, such as areas, useful in computing the

quantization of the degree of stenosis by consequence Obtaining a structured object, easy to handle. Finally, the most important advantage in terms of execution time (about 5 seconds).

The result obtained by Birkeland et al. [10] between 7-10 minutes and Hua et al. [11] provides offers an innovative approach to segmenting tubular structures with a calculation time is less than 2 min. On the other hand, the execution time of our proposed algorithm of the order of several seconds. Thus, the proposed algorithm is faster than the other two methods.

This comparison also shows that our method can correctly follow nearly all branches and also reduce the execution time while having the ability to segment the thin vessels.

7. Conclusion:

We propose in this work a method to implicitly represent the 3D model of a vascular tree from the image of the human retina. We also describe algorithms to extract the 2D vascular tree of the human retina that allows us to exploit the different features the retina images and data mining (endpoint, branch points and the points of the center line), the results of this step are converted into control points that are easy to store and handle in the next step. Then we apply the interpolation algorithm for this data, we proposed an automatic algorithm for modeling a smooth curve with linear spline, least square, and cubic spline interpolation. The result given by the least squares method gives rise to a significant error. The result given by the least squares method gives rise to a significant error. Indeed, the RMS value is about 0.7 pixels and the maximum error is about 1.9 pixels. However, the interpolation errors disappear by using a linear or cubic spline. In the last step, we present a 3D reconstruction method for a network of tubular structures. Generalized cylinders follow the curves of ships interpolated using the Generalized Right Cylinder State Model method that gives us a model consists of two geometric objects: a generator axis H and a surface S. The results clearly show the feasibility and speed of the method proposed. Our method combines the sequential approach vessel tracking, with the use of a continuous model of a generalized cylinder.

8. References

- [1]. M. Spiegel, T. Redel, T. Struffert, J. Hornegger and A. Doerfler. "A 2D driven 3D vessel segmentation algorithm for 3D digital subtraction angiography data". *Physics in medicine and biology*. 56, pp. 6401–6419. 2011.
- [2]. Alejandro F. Frangi, Wiro J. Niessen, Romhild M. Hoogeveen, Theo van Walsum, and Max A. Viergever."Model-Based Quantitation of 3-D Magnetic Resonance Angiographic Images". *IEEE Transactions on medical imaging*, VOL. 18, NO. 10, OCTOBER 1999.
- [3]. L. Antiga, B. Ene-Iordache, L. Caverni, et al., "Geometric reconstruction for computational mesh generation of arterial bifurcations from CT angiography", *Computerized Medical Imaging and Graphics*, volume 26, pp. 227-235, 2002.
- [4]. S. Aylward, E. Bullitt, S. Pizer, D. Eberly, "Intensity ridge and widths for tubular object segmentation and description", *Proc. IEEE Math. Meth. Biomed. Image Anal.*, pp. 131-138, 1996.
- [5]. C. Bauer, H. Bischof, "A novel approach for detection of tubular objects and its application to medical image analysis", *In DAGM Symposium on Pattern Recognition*, pp. 163-172, 2008.
- [6]. C. Bauer, T. Pock, H. Bischof, R. Beichel, "Airway tree reconstruction based on tube detection. In International Workshop on Pulmonary Image Analysis", *Medical Image Computing and Computer Assisted Intervention*, pp. 203-213, 2009.
- [7]. C. Bauer, T. Pock, E. Sorantin, H. Bischof, R. Beichel, "Segmentation of interwoven 3d tubular tree structures utilizing shape priors and graph cuts", *Medical Image Analysis*, Vol. 14, pp. 174-184, 2010.
- [8]. M. de Bruijne, B. van Ginneken, W. Niessen, M. Viergever, "Adapting active shape models for 3D segmentation of tubular structures in medical images", *In Proc. Inf. Process. Med. Imaging*, pp. 136-147, 2003.

- [9]. M. Jourdain, J. Meunier, J. Sequeira, J. M. Boi, and J. C. Tardif, "A robust 3D IVUS transducer tracking using single-plane Cineangiography", *IEEE Transactions on Information Technology in Biomedicine*, Vol. 12, Issue 3, pp. 307-314, May 2008.
- [10]. A. Birkeland, D. M. Ulvang, K. Nylund, T. Hausken, O. H. Gilja, and I. Viola, "Doppler-based 3D Blood Flow Imaging and Visualization", *SCCG'13 Proceedings of the 29th Spring Conference on Computer Graphics*, pp. 115-122, New York, NY, USA, 2013.
- [11]. L. Hua, A. Yezzi, "Vessels as 4-D Curves: Global Minimal 4-D Paths to Extract 3-D Tubular Surfaces and Centerlines", *IEEE TRANSACTIONS ON MEDICAL IMAGING*, VOL. 26, NO. 9, pp. 1213-1223, SEPTEMBER 2007.
- [12]. B. Avants, J. Williams, "An Adaptive Minimal Path Generation Technique for Vessel Tracking in CTA/CE-MRA Volume Images", in : *MICCAI '00 : Proceedings of the Third International Conference on Medical Image Computing and Computer-Assisted Intervention*, Springer-Verlag, London, UK, ISBN 3-540-41189-5, pp. 707-716, 2000.
- [13]. C. Boldak, Y. Rolland, C. Toumoulin, et al., "An improved model based vessel tracking algorithm with application to Computed Tomography Angiography", *Biocybernetics And Biomedical Engineering*, volume 23, no. 1, pp.41-63, 2003.
- [14]. C. Castro, M. A. Luengo-Oroz, A. Santos, M. J. Ledesma-Carbayo, "Coronary artery tracking in 3D cardiac CT images using local morphological reconstruction operators". *The Midas Journal*, 2008.
- [15]. J. Azencot, M. Orkisz, "Deterministic and stochastic state model of right generalized cylinder (RGC-sm): application in computer phantoms synthesis", *Graphical Models*, volume 65, no. 6, pp. 323-350, doi: 10.1016/S1524-0703(03)00073-0, 2003.
- [16]. S. Shafer, "Shadows and silhouettes in computer vision", *The Kluwer International Series in Engineering and Computer Science*, Kluwer Academic, Boston/ Dordrecht/Lancaster, 1985.
- [17]. O. Wink, W. Niessen, A. Frangi, et al., "3D MRA coronary axis determination using a minimum cost path approach", *Magnetic Resonance in Medicine*, volume 47, no. 6, pp. 1169-1175, 2002.
- [18]. J. Yi, J. Ra, "Vascular segmentation algorithm using locally adaptive region growing based on centerline estimation", *Medical Imaging 2001 : Image Processing*, volume 4322, no. 1, pp. 1329-1336, 2001.
- [19]. C. Pisupati, L. Wolff, W. Mitzner, et al., "A Central Axis Algorithm for 3D Bronchial Tree Structures", *IEEE International Symposium on Computer Vision*, pp. 259-264, 1995.
- [20]. S. Aylward, E. Bullitt, "Initialization, Noise, Singularities, and Scale in Height Ridge Traversal for Tubular Object Centerline Extraction", *IEEE Transactions on Medical Imaging*, volume 21, no. 2, pp. 61-75, 2002.
- [21]. S. Bouix, K. Siddiqi, A. Tannenbaum, "Flux driven automatic centerline extraction", *Medical Image Analysis*, 9(3), pp. 209-221, 2005.
- [22]. E. Dikici, T. O'Donnell, L. Grady, R. Setser, R. D. White, "Coronary artery centerline tracking using axial symmetries". *The Midas Journal*, 2008.
- [23]. M. E. Gegúndez-Arias, A. Aquino, J. M. Bravo and D. Marín. "A Function for Quality Evaluation of Retinal Vessel Segmentations". *IEEE transactions on medical imaging*, VOL. 31, NO. 2, February 2012.
- [24]. A. Hoover, V. Kouznetsova and M. Goldbaum. "Locating Blood Vessels in Retinal Images by Piecewise Threshold Probing of a Matched Filter Response". *IEEE transactions on medical imaging*, VOL. 19, NO. 3 March 2000.
- [25]. STARE (STRUCTURED Analysis of the Retina) project website, <http://www.ces.clemson.edu/~ahoover/stare>.
- [26]. E. Zhang, Y. Zhang and T. Zhang. "Automatic retinal image registration based on blood vessel feature point". *Proceedings of the First International Conference on Machine Learning and Cybernetics, Beijing*, 4-5 November 2002.

- [27]. N. K. El Abbadi and E. H. El Saadi, "Automatic Detection of Vascular Bifurcations and Crossovers in Retinal Fundus Image", *IJCSI International Journal of Computer Science Issues*, Vol. 10, Issue 6, No 1, November 2013.
- [28]. R. Shahzad, H. K. li, C. Metz, H.Tang, M. Schaap, L. van Vliet, W. Niessen and T. van Walsum, "Automatic segmentation, detection and quantification of coronary artery stenoses on CTA", *Int J Cardiovasc Imaging*, 29, pp. 1847,1859 ,2013.
- [29]. C. de Boor, "On the Convergence of Odd-Degree Spline Interpolation", *Journal of approximation theory 1*, pp. 452-463, 1968.
- [30]. J. H. Ahlberg, E. N. Nilson, and J. L. Walsh, "The Theory of Splines and Their Applications", Mathematics in Science and Engineering, Volume 38. XI + 284 S, New York/London 1967.
- [31]. E. W. Chesey, F. Schurer, "A Note on the Operators Arising in Spline Approximation", *Journal of approximation theory 1*, pp. 94-102, 1968.
- [32]. C. A. Hall, "On Error Bounds for Spline Interpolation", *Journal of approximation theory 1*, pp. 209-218, 1968.
- [33]. T. R. Lucas, "Error Bounds for Interpolating Cubic Splines under Various End Conditions", *SIAM Journal on Numerical Analysis*, Vol. 11, No. 3, pp. 569-584, Jun 1974.
- [34]. R.E.Deakin, D.G.Kildea, "A note on standard deviation and rms", *The Australian surveyor*, Vol. 44, No. 1, pp. 74-79 , june 1999.



Hichem Guedri received his Master in electronic from Monastir University of Faculty of sciences in 2010. Currently, he has been a Ph.D. student in electronic and his Ph.D. from the same Faculty. His Ph.D. project is devoted to the development of a fractal model for three-dimensional reconstruction of the retinal vasculature. Currently, he has been a contractual assistant in Faculty of Sciences Monastir and he is a member of Electronic and Microelectronic Research Group.



Fraj Echouchene received his PhD in physics from Faculty of Science of Monastir, Tunisia in 2011. His PhD project is devoted on the numerical simulation of cavitating flows. Currently, he is an assistant professor in Faculty of Science of Gafsa and he is a member of the Laboratory of Electronics and Microelectronics.



Hafedh Belmabrouk has received a PhD degree (1992) in Laser Doppler Velocimetry from Ecole Centrale de Lyon (France). He currently supervises a team of about 20 researchers in the field of Non Linear Optics, Biosensor and Micro fluidics, and Heat Transfer in nanodevices.